

Roughness Influence on Initiation of Fretting Fatigue Scar of Ti-6Al-4V Alloy

Capitanu L.¹, Badita L.L.², Florescu V.³, Tiganesteanu C.¹

¹*Institute of Solid Mechanics of the Romanian Academy 010141, Bucharest, Romania*

²*National Institute of Research and Development for Mechatronics & Measurement Technique, 021631, Bucharest, Romania*

³*University of Civil Engineering, 020396, Bucharest, Romania*

lucian.capitanu@yahoo.com¹, badita_l@yahoo.com², florescuvirgil@yahoo.com³, tctin@yahoo.com¹

Abstract: This paper reports on the experimental studies undertaken to detect the early stage when appears the fretting wear of the Ti-6Al-4V alloy used for the hip prostheses. Wear is a critical aspect for estimating the fretting fatigue. Studies were performed on samples of special shape, in order to be able to study the influence of in contact surfaces roughness on the durability to fretting. Fretting buffers, with roughnesses R_a of the contact surface of 0.015 and 0.045 μm , and Ti-6Al-4V samples with roughnesses $R_a = 0.045 \mu\text{m}$, $R_a = 0.075 \mu\text{m}$ and $R_a = 0.19 \mu\text{m}$, were used. Testing periods of 3 seconds, 1 minute and 5 minutes were selected to capture the moment of the fretting scar appearance, long before these initiate the eventual fretting cracking. Simultaneously with fretting wear of the surface, the friction coefficient was also measured. From the in time evolution determinations of the fretting wear, it resulted that, under the experimental conditions used, the minimum wear occurs at a certain value of the roughness and not at the minimum roughness. Surprisingly, the minimum friction coefficient does not coincide with the minimum fretting wear.

Keywords: Ti-6Al-4V alloy, roughness, fretting damage, wear, friction

1. Introduction

Fretting is a phenomenon that occurs at the interface between two bodies in contact, which are pressed against each other in the presence of cyclic load, which gives rise to a small relative displacement. At the interface there is a complex interaction between wear, corrosion and fatigue. Thus, this phenomenon involves many aspects of contact mechanics, multiaxial fatigue, tribology, and materials science. Directly or indirectly, the damage due to the fretting fatigue is caused by several factors and interdependent variables, such as the amplitude of the relative displacement, normal load, tangential and axial loads, material's nature, friction coefficient, cyclic frequency, temperature and the environment.

There are several application domains where this phenomenon occurs, such as aerospace industry, human body implants, automobiles, etc. Designing at fatigue without considering the effect of fretting will certainly lead to premature and unexpected failure in many applications.

Fretting can be classified into two categories: fretting fatigue and fretting wear. Also, corrosion, mentioned in several studies as the third manifestation of the fretting [1], was accepted in the whole



area of fretting damage and incorporates the two manifestations of fretting fatigue and fretting wear [2].

In recent years, several studies have used multiaxial fatigue models to establish correlations with the experimental data of fretting fatigue. The most common multiaxial fatigue models are: Dang Van (DV), Smith-Watson-Topper (SWT) and Fatemi and Socie (FS) [2-7]. Lykins et al. [6] investigated the behavior of fatigue crack initiation by fretting of the titanium alloy, Ti-6Al-4V, using the SWT parameter.

Tribo-corrosion continued to be an area of many investigations. In particular, the concepts and influence of the third body during the tribo-corrosion processes, as well as the significance of the experimental techniques for studying problems caused by tribo-corrosion, have been investigated. A typical tribo-corrosion action is the materials degradation due to mechanical, electrochemical and synergistic effects. These effects are distinct areas of scientific study, but they occur together to cause the wear of a material. A typical example of mechanical experiment includes measurements of tangential load. However, some electrochemical investigations have been performed to help understand the synergistic effects. These synergies have been analyzed to help understand corrosion, both as a mechanical phenomenon and as a mechanical-electrochemical coupled phenomenon [8].

To predict the crack's propagation in a fretting wear case, Fidrici et al. [9] also used the SWT parameter. Moreover, to match the predicted life with the experimental life, a new factor has been added that takes into account the effect of the residual compression stresses induced by the striking blow. Araujo and Nowell [10] have demonstrated that the use of the SWT and FS approaches to estimate the life of fretting fatigue initiation of Ti-6Al-4V is not appropriate if the calculations are based exclusively on the stress-strain behavior of the surface at extremely tensioned points. This suggested that these methods would not be adequate for assessing the life of fretting fatigue initiation in tests with different geometries, and that the reason for the poor performance of the prediction methodology is the presence of the effects of the high stress gradient. They proposed two methods of averaging, which, combined with a multiaxial fatigue criterion, would give a less conservative prediction of the life of fretting fatigue initiation. The first method is an average of the SWT and FS parameters over a characteristic depth on the critical plane. The second method is an average of the stresses in a characteristic elementary volume. Both methods of calculating the average produced sensible similarly results.

Giannakopoulos et al. [11] reported that the fretting problem can be approached as a problem of simple fatigue subjected to a localized stress concentration. They developed an analytical model for fretting fatigue at a corner of a rounded mandrel in contact with a substrate, and an analogy with the initiation of the fatigue crack at the notch of a tip was made. They analyzed the similarities and differences between the stress concentration factors at the edge of the mandrel-on-flat unexpectedly rounded contact and the tip of a blunt crack. Notch-like methodology provided a direct connection between the life of the fretting fatigue crack initiation of a flat mandrel with rounded corners and the life of the simple fatigue crack initiation of a smooth sample made of the same material. Model predictions were compared to the fretting fatigue experiments on Ti-6Al-4V showing good concordance.

Madge et al. [12] have shown that the wear is a critical aspect for estimating the fretting fatigue and can have a major effect on the predicted evolution of the stresses and deterioration parameters (e.g. SWT), and, thereafter, on the predicted fatigue life and the position's failure. They performed a finite elements simulation (removed element simulation), which simultaneously combines a fretting wear model and the SWT parameter of fretting fatigue, which includes the effect of the stress peak.

From the various approaches mentioned above, one can conclude that is still missing a more comprehensive analysis of the fretting fatigue phenomena. The data currently available on different materials and test conditions are insufficient to allow taking a decision on a suitable model.

The models chosen for examination are two models of fatigue based on deformation. The first approach is the SWT model, and the second approach is Morrow's model. The first model is already used in fretting fatigue, while the latter was first tested for fretting fatigue situations by Buciumeanu et al., [1]. In both models, the effects of average stress are included. Morrow's model was modified to introduce the local stresses involved in the fretting fatigue process (normal, tangential and axial).

Moreover, a new parameter, which is a stress concentration factor, K_f , which includes the effect of the affected area, called here, the "effect of the fretting scar", has been introduced in both models.

In accordance with the direction of relative movement under a ball-on-flat (BOF) contact configuration, four basic fretting modes can be distinguished, namely: tangential, radial, rotational and torsional fretting. Rotational fretting can be defined as the relative movement induced by the micro-amplitude rotation that takes place in the pair of contacts with tightly fixing in the alternative loading medium. Rotational fretting phenomena resulting in wear of the contact surface exist in many mechanical equipment and instruments such as cars, rail vehicles, planes and biomedical implants, and wear greatly induces the reduction of component life, and huge economic losses. Researches on rotating fretting wear under the BOF contact configuration were performed by Zheng et al., [13]. However, the contra-pair contact configurations, in which the fretting damage occurs in practice, are often not BOF contacts, but also other contact configurations. According to the modern tribological theory, the behaviors of contact stress, of contact stiffness and of contact residues are quite different under different contact configurations. The contact configuration plays a very important role in the fretting wear. In order to understand the rotating fretting mechanisms in the different contact configurations, rotating fretting tests with ball-on-concave (BOC) and ball-on-flat (BOF) contacts were performed at the same maximum contact stress and, respectively, normal loads.

Many research works have been done on the wear mechanisms by fretting and fatigue. It has been achieved the understanding of some basic mechanisms of fretting, allowing the development of various possible palliatives. However, to date, there has been no general agreement on the mechanisms and modeling of fretting. For example, the mechanical, chemical, tribological and electrical processes between the two contact surfaces during the fretting were not fully understood, because the most models and wear theories are based on the observation of deterioration by the fretting wear. The direct or in situ observation of the fretting wear process implies the procurance of some time-dependent changes and casts more light on the actual fretting mechanisms [14]. Fretting, in a total hip prosthesis, results from the destruction of the passive oxide layer from the metal, thus leading to increased corrosion and to the residues generation, such as polymer and/ or metal oxides particles resulting in serious dysfunctions of the hip joint [15]. The cyclic loading due to the daily human walking, and the differences between the mechanical properties of the femoral stem and bone cement give rise to the separation of the two materials. This unsoldering leads to secondary effects, such as degradation and cracking of cement. Residues, including metal oxides and ions, invade bone tissues through cracks and finally induce inflammation in the bone tissues

This study presents the experimental and theoretical research on the fretting behavior of the Ti-6Al-4V alloy samples used for the manufacture of total hip prostheses.

2. Experimental evaluation

2.1. Experimental assembly for testing

Fretting tests were performed on a universal servo-hydraulic testing machine, MTS Bionix, figure 1.

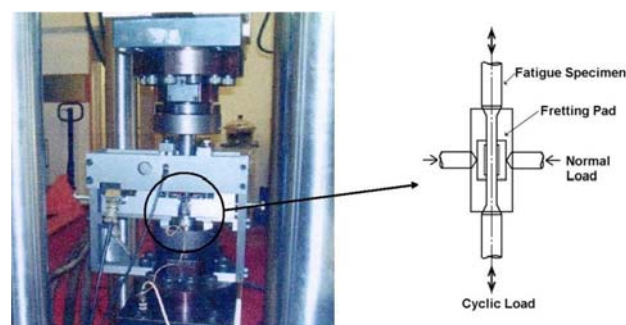


Figure 1. MTS Bionix servo-hydraulic dynamic testing machine

The testing machine allowed application of a 600 kN load under static conditions and 500 kN for fatigue loading. The maximum cyclic loading frequency of the machine is 50 Hz. The equipment operates at ambient temperature in the laboratory environment. To perform fretting fatigue tests, on the machine was a special fretting device that has two load cells that allow (prior to testing) application of normal and tangential contact loads (during the test) and their recording/ measurement. A 1000 N loading cell is used to set and measure the pre-tangential/ tangential load and a 2500 N loading cell to set/ measure the normal load. The load is applied by two buffers, which are pressed perpendicularly on the flat faces of the sample by a pair of compression springs, which are loaded with adjustable screws. Also, two vertical compression springs, which action on the buffer, are used to apply the pre-tangential load (to avoid the buffer's movement).

"Bridge" type fretting buffers were used, which have as main advantage the simplicity with which a normal fatigue specimen can be used, both at bending and at cyclic traction. The bridges are simply fixed to the sides of the specimen by a ring or a similar arrangement and the cyclic deformation of the specimen causes a relative movement between the bridge legs and the specimen.

The buffers were made of RUL 1 bearing steel, hardened and rectified to a roughness R_a of 0.15 μm . The tangential load varies depending on the axial load of the machine. Due to the system's symmetry, loads are measured only in one part. The axial cyclic load applied to the sample was monitored with the machine's loading cell.

2.2. The geometry of the sample and buffer

Fretting fatigue experiments were performed using the geometries of sample and buffer, which are shown in figure 2, and figure 3 shows the scheme of the sample-buffer contact test configuration.

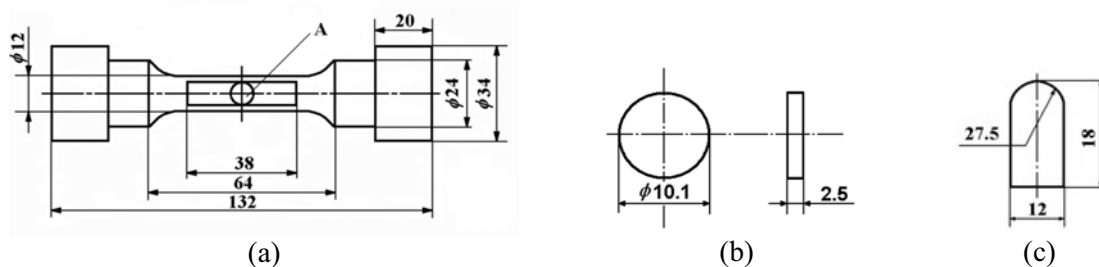


Figure 2. Geometry of the specimen, sample and fretting test buffer.

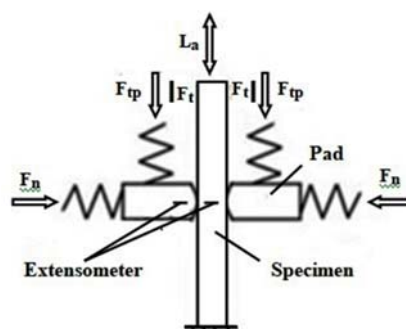


Figure 3. Scheme of the test configuration of the sample-buffer contact: F_n – normal loading of the buffer; F_{tp} – tangential pre-loading of the buffer; F_t – tangential loading of the buffer and L_a – axial load of the machine.

The specimen (figure 2) has a special shape, with two flat opposite faces (A), milled, rectified and polished in the middle of the sample. In this situation, the two contact areas on the flat sides of the sample were generated. In the middle of these areas, holes with diameter of 10.1 mm and depth of 2.5 mm were drilled. Fretting samples were introduced into these places. This was done in order to study

the influence of in contact surfaces roughness to the durability at fretting. Several buffers and fretting samples were produced, which had been finished with roughness $R_a = 0.015 \mu\text{m}$. The spherical head of the buffers had a roughness of $0.05 \mu\text{m}$. Prior to testing, the samples and buffers surfaces were ultrasonically cleaned in alcohol. Figure 3 schematically shows the configuration of the sample-buffer contact testing in the fretting fatigue tests.

2.3. Experimental procedure

Under static conditions, the compressive stresses due to point contact, p_{max} and p_{med} (maximum and average contact pressure) are given by:

$$p_{max}^3 = 1.5 PE^2 / \pi r^2 (1 - \mu^2)^2 \quad (1)$$

$$p_{med} = \frac{P}{\pi a^2} \quad (2)$$

while the radius a of the circular contact surface is:

$$a^3 = 1.5(1 - \mu^2)P \frac{r}{E} \quad (3)$$

where P is the load; a the radius of the contact surface and r the radius of the spherical head of the buffer.

For coupling components made of steel, the values of the previous equations become:

$$p_{max} \approx 5800 \sqrt[3]{P} \quad (4)$$

$$p_{med} \approx 1700 \sqrt[3]{P} \quad (5)$$

$$a \approx 0.09 \sqrt[3]{P} \quad (6)$$

Particular attention was given to the finishing of the specimens friction surfaces. The state of the surface, being defined by topography, microstructure of the superficial layer and the oxidation state, has a major contribution to the wear process. Due to the complexity of surface creation through an abrasion process, the safest way to ensure a consequent reproducible surface is strictly by adhering to all stages of the finishing process.

The following stages have been established: shape transformation, finishing transformation, thermal treatment, rectification, fine adjustment and ultimately super-finishing of the work surface. While in all the stages, until the fine final adjustment, traditional manufacturing techniques are used, it is worth mentioning that the overall intensity of the process is deliberately maintained at a low level to protect the superficial structure of the material. The super-finishing stage uses the metallographic polishing techniques and includes: wet polishing with abrasive paper of $32 \mu\text{m}$ and $17 \mu\text{m}$ granulation, polishing with diamond paste of $6 \mu\text{m}$ and $1 \mu\text{m}$ granulation, and, finally, wet polishing using alumina suspension that has a granulation of 2000 \AA . The surfaces are then cleaned with alcohol and distilled water and then are dried. The storage of the finished samples is done in sealed containers on a layer of silica gel.

After the super-finishing stage, four different roughness values were obtained for Ti-6Al-4V samples surfaces: $R_a = 0.015 \mu\text{m}$, $R_a = 0.045$, $R_a = 0.075 \mu\text{m}$ and $R_a = 0.190 \mu\text{m}$. Surfaces roughness was determined using a profilometer with parametric transducer and graphical recording, Perth-O-Meter. The tool allows not only the recording of surface profiles, but also the determination of the R_a and $r.m.s$ values, defined as:

$$R_a = \frac{1}{l} \int_0^l |y| dx \quad (7)$$

$$r.m.s = \left(\frac{1}{l} \int_0^l y^2 dx \right)^{1/2} \quad (8)$$

The tests mainly followed the evolution of fretting scar according to the normal load applied under different roughness conditions of the surface and normal loading, but at constant tangential loading. Experimental tests were performed under lubrication conditions with SBF (simulated body fluid) from Hyclone Inc., USA, which has a composition close to that of the human serum.

3. Experimental results

Fretting fatigue tests were performed at a stress ratio $R = 0.1$ where $R = F_n / F_t$. All tests were performed at ambient temperature, in the laboratory environment, as well as at a cyclic frequency of 4 Hz. The profiles and microphotographs of the initial surfaces topography with initial roughness $R_a = 0.015 \mu\text{m}$ (A1-A2), $R_a = 0.045 \mu\text{m}$ (A3-A4), $R_a = 0.075 \mu\text{m}$ (A5-A6) and $R_a = 0.19 \mu\text{m}$ (A7-A8) are illustrated in figure 4.

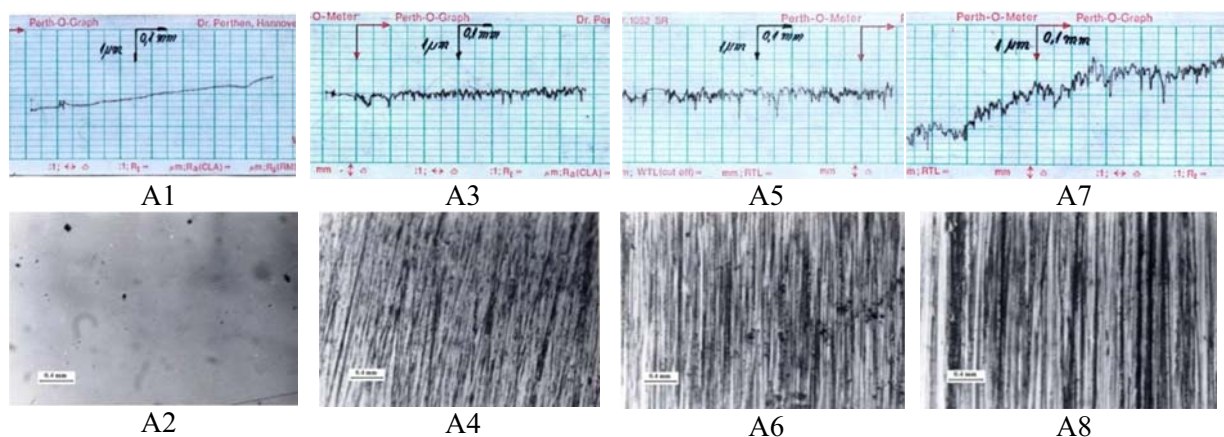


Figure 4. Profiles and microphotographs of the initial surfaces topography with roughness $R_a = 0.015 \mu\text{m}$ (A1-A2), $R_a = 0.045 \mu\text{m}$ (A3-A4), $R_a = 0.075 \mu\text{m}$ (A5-A6) and $R_a = 0.19 \mu\text{m}$ (A7-A8).

In order to properly view the wear of the fixed surface, depending on the roughness of the coupling, the following solution was used: the coupling asperities were concentrated on one of the surfaces, especially on the mobile one. Fixed surface has always had the minimum achievable roughness, i.e. approximately $R_a \approx 0.015 \mu\text{m}$. As is well known, the composite roughness of the coupling, expressed by standard deviations, σ , is:

$$\sigma^2 = \sigma_1^2 + \sigma_2^2 \quad (9)$$

where σ_1, σ_2 represent the standard deviations of the two surfaces.

If one of the surfaces has a much smaller roughness, i.e. $\sigma_1 \ll \sigma_2$, then $\sigma \approx \sigma_1$. Thus it is possible to study the influence of roughness on wear, even by changing the roughness of a single surface. In these conditions and under a load $P = 30 \text{ N}$, the relative velocity $u = 1.74 \text{ m/s}$ and at the temperature $\theta = 50^\circ\text{C}$ of the lubricant volume, the evolution of the surface wear was developed in function of time for the following roughnesses of the mobile surface: $R_a = 0.015 \mu\text{m}$; $R_a = 0.045 \mu\text{m}$; $R_a = 0.075 \mu\text{m}$ and $R_a = 0.19 \mu\text{m}$.

3.1. Evolution of the contact surface state in fretting conditions

The consequence of fretting is the fretting scar that forms in the area of the buffer-sample contact and which can evolve by initiating the fretting crack until the sample breaks over time. The initiation phase takes almost 80% of the coupling's runtime. In figure 5, some fretting wear scars obtained under the above mentioned conditions (at time $t = 5$ min) are shown selectively to estimate the reproducibility of the results.

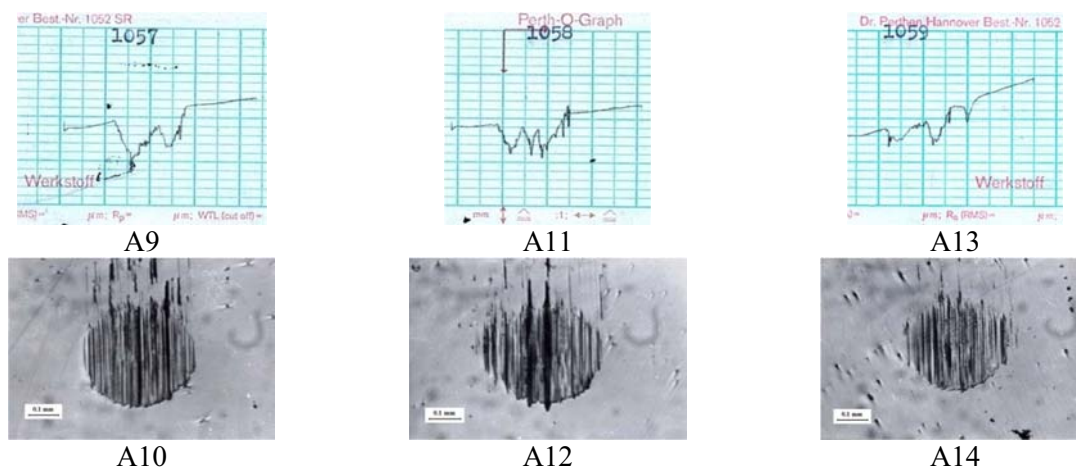


Figure 5. Central transversal profile and image of fretting wear scar. $R_a = 0.015 \mu\text{m}$, $t = 5$ min.

The scar volume for the three experimental determinations is: 1057 specimen: $V = 8.50 \times 10^{-5} \text{ mm}^3$; 1058 specimen: $V = 6.11 \times 10^{-5} \text{ mm}^3$; 1059 specimen: $V = 4.00 \times 10^{-5} \text{ mm}^3$, resulting an average volume $\bar{V} = 6.2 \times 10^{-5} \text{ mm}^3$. For wear measurements, a deviation of 25% is completely satisfactory. Figure 6 shows the evolution of the wear depending on time, for the roughness of the buffer $R_a = 0.045 \mu\text{m}$. Trial times of 3 seconds, 30 seconds, 1 minute and 5 minutes were selected, each performed with another coupling. This solution was chosen to also monitor the change of the buffer surface state. Figure 6 shows that, except for the first 5 minutes, the wear remains at the same level.

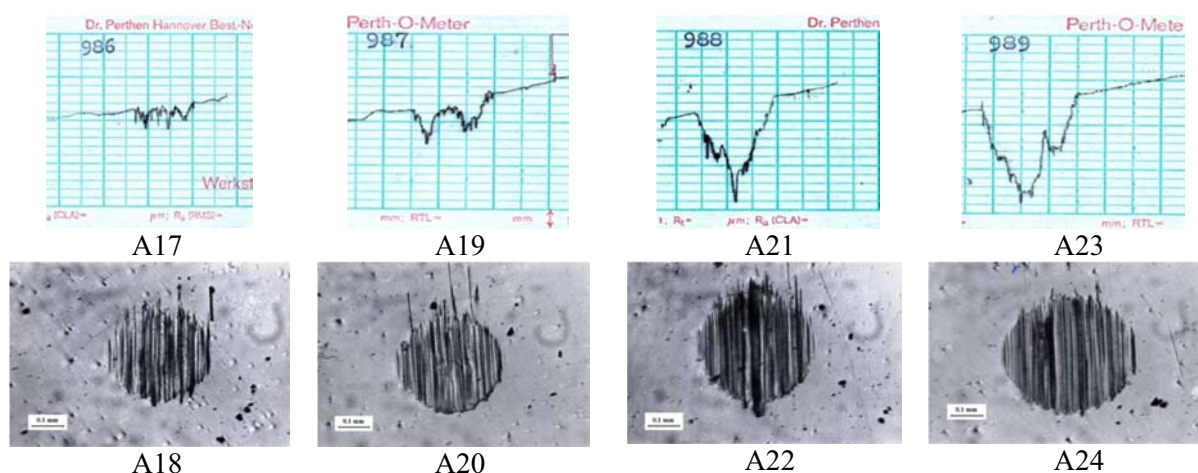


Figure 6. Central transversal profile and image of fretting wear scar $R_a = 0.045 \mu\text{m}$, $t = 5$ min.

In figure 7 is shown the transversal profile and the image of the fretting wear scar for the sample with $R_a = 0.045 \mu\text{m}$, $t = 5$ min (sample 703); $R_a = 0.045 \mu\text{m}$, $t = 5$ min, but with the buffer from the previous determination (total operating time $t = 10$ min, sample 704); $R_a = 0.045 \mu\text{m}$, $t = 5$ min, with the buffer from the previous determination (total operating time $t = 20$ min, sample 705).

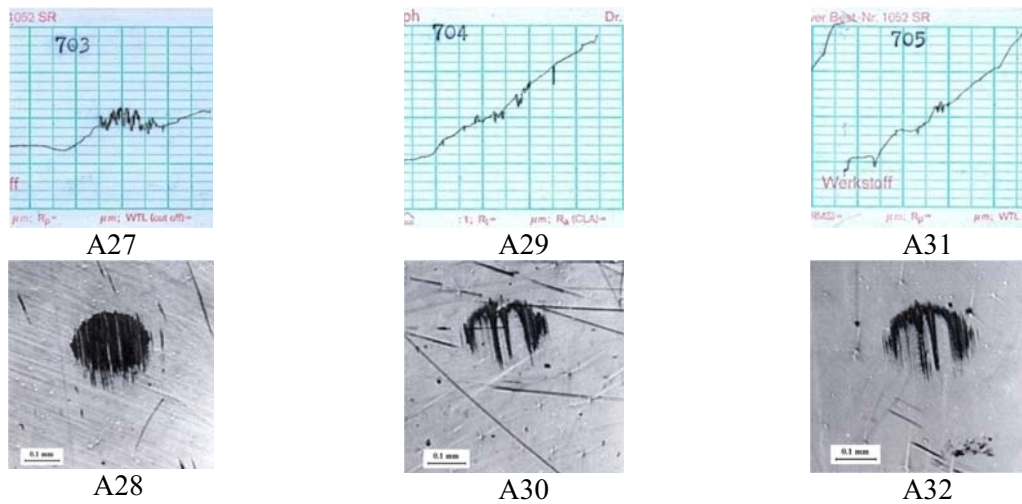


Figure 7. Profile and image of the fretting wear scar for samples with $R_a = 0.045 \mu\text{m}$, $t = 5 \text{ min.}$ (sample 703); $R_a = 0.045 \mu\text{m}$, $t = 5 \text{ min.}$, with the buffer from the previous determination (total operating time $t = 10 \text{ min.}$ (sample 704); $R_a = 0.045 \mu\text{m}$, $t = 5 \text{ min.}$, with the buffer from the previous determination–total operating time $t = 20 \text{ min.}$ (sample 705).

The evolution of fretting wear depending on time for different roughnesses is presented in the double-logarithmic diagram in figure 8.

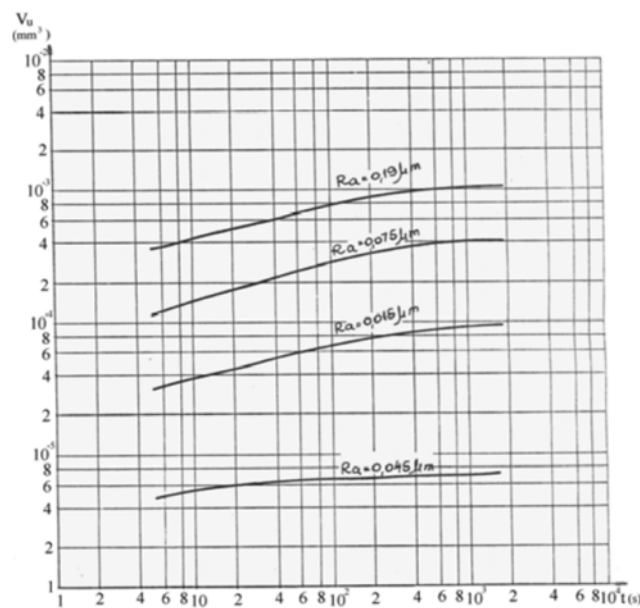


Figure 8. Evolution of wear versus time, for different roughness R_a .

By increasing the operating time from 5 minutes to 30 minutes, the wear increases by only about 10%. It is worth noting the rapid reduction of the wear velocity over time, excepting the surface with roughness $R_a = 0.045 \mu\text{m}$. In the first 3 seconds, between 25% and 50% of the wear occurs in 30 minutes. This evolution of wear is explained by the surfaces running, which leads to a change in the lubrication regime. Note that the amount of wear on the plate is caused by the initial wear (in the first few seconds of operation). This observation allows the use of the wear value at $t = 5 \text{ min}$ as a representative quantity for the existing operating conditions. During this operation period, the values scattering is small.

In the case of surfaces with $R_a = 0.045 \mu\text{m}$, the wear is so low that during the entire period of time used, the lubrication conditions remain roughly unchanged.

The evolution of the fretting wear function of time, for roughness $R_a = 0.075 \mu\text{m}$ (samples 829, 830 and 832) is shown in figure 9.

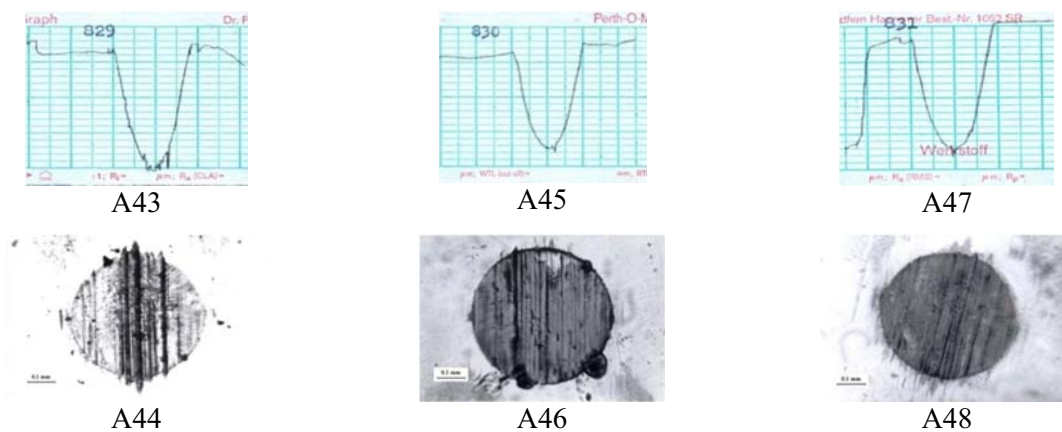


Figure 9. Evolution of the fretting wear function of time, for $R_a = 0.075 \mu\text{m}$ (samples 829, 830, 832).

Different roughnesses used have caused not only a difference between the amount of wear volume of the scar, but also of the wear scar appearance (the type of wear). In the case of the surfaces with $R_a = 0.015 \mu\text{m}$, $R_a = 0.075 \mu\text{m}$ ($t = 3 \text{ s}$) and $R_a = 0.19 \mu\text{m}$ ($t = 3 \text{ s}$), the wear is of adhesive type (metallic shape with pronounced scratches). In the case of surfaces with $R_a = 0.045 \mu\text{m}$, the fretting wear type is predominantly oxidative. While the fretting wear velocity is reduced due to surface conformation, the surfaces with $R_a = 0.075 \mu\text{m}$ and $R_a = 0.19 \mu\text{m}$ also undergo in oxidative wear regime.

The evolution of the fretting wear function of time, for roughness $R_a = 0.19 \mu\text{m}$ (samples 835, 849, and 850) is shown in figure 10.

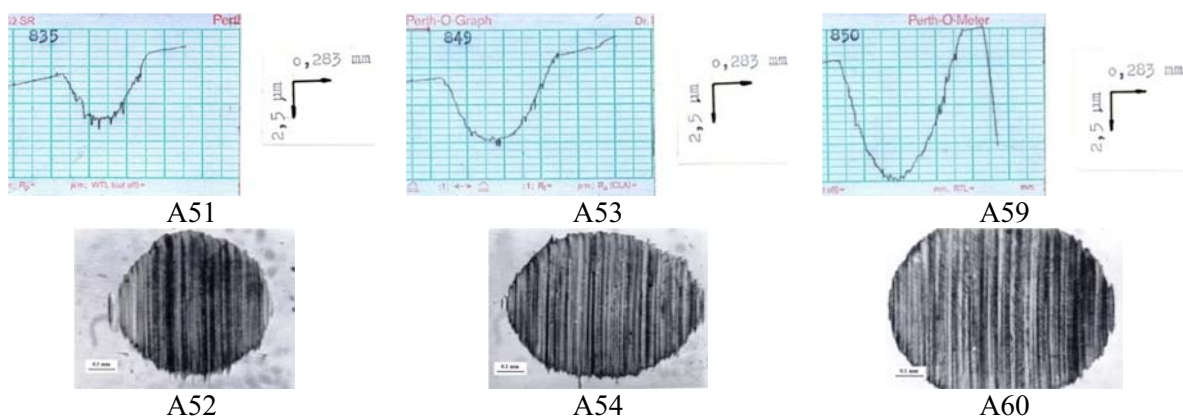


Figure 10. Evolution of the fretting wear function of time, for roughness $R_a = 0.19 \mu\text{m}$ (samples 835, 849, and 850).

For the roughnesses $R_a = 0.015 \mu\text{m}$, $R_a = 0.075 \mu\text{m}$ and $R_a = 0.19 \mu\text{m}$, the results obtained for the volume of the worn material are in accordance with the contact deformation, determined by the parameter of the lubricant film h_{min} / σ . For surfaces with roughness $R_a = 0.045 \mu\text{m}$, an influence of the running-in was observed. After the first 5 minutes of operation, the entire contact surface is covered with oxide. The scar obtained after another 5 minutes, with the same buffer, has a special shape, the oxidative wear area is limited to half of the loaded surface (samples A52 and A54).

Figure 11 shows the central profile and the image of the fretting wear scar $R_a = 0.19 \mu\text{m}$, $t = 30 \text{ min}$, sample 997 (new buffer).



Figure 11. Central transversal profile and image of wear scar. $R_a = 0.19 \mu\text{m}$, $t = 30 \text{ min.}$, sample 997, (new buffer).

Next, figure 12 shows the effect of the running-in on the fretting wear behaviour of the surface with $R_a = 0.19 \mu\text{m}$, with the same buffer as in the previous test, compared to figure 13, that shows the effect of the running-in on the wear behavior of the surface with roughness $R_a = 0.045 \mu\text{m}$, using a new buffer.



Figure 12. The effect of running-in on the fretting wear behaviour of the surface with $R_a = 0.19 \mu\text{m}$, $t = 5 \text{ min}$, sample 998. The buffer from previous determination was used.

In the experimental conditions of figures 11 and 12, it is clearly observed the start of the fretting scars elongation in the sliding direction (from top to bottom A61 / A62 and A63 / A64) and the typical W-shape of the transversal profile of the scar, noted in many of the papers published in the field [16-20]. Different roughnesses used have caused not only a difference between the values of the fretting worn volume, but also of the wear scar appearance (type of wear). In the case of surfaces with $R_a = 0.015 \mu\text{m}$, $R_a = 0.075 \mu\text{m}$ ($t = 3 \text{ s}$) and $R_a = 0.19 \mu\text{m}$ ($t = 3 \text{ s}$), the wear is of adhesive type (metallic shape with pronounced scars). In the case of surfaces with $R_a = 0.045 \mu\text{m}$, the predominant type of wear is the oxidative one. While the wear velocity is reduced as a result of the surface conformation, surfaces with $R_a = 0.075 \mu\text{m}$ and $R_a = 0.19 \mu\text{m}$ also go under oxidative wear regime. In the case of super-finished surfaces with $R_a = 0.015 \mu\text{m}$ no favorable influence of the running-in is observed. For surfaces with roughnesses of $R_a = 0.045 \mu\text{m}$, a favorable influence of the running-in was observed (figure 13).

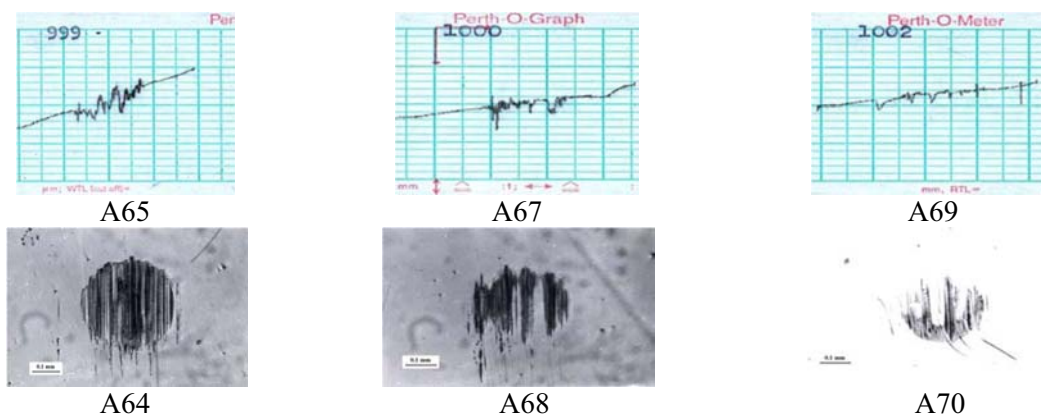


Figure 13. The effect of the running-in on the fretting wear behaviour of the surface with $R_a = 0.045 \mu\text{m}$, $t = 5 \text{ min}$, samples 999 (with new buffer), 1000 and 1002 (with the buffer from the previous determination).

After the first 5 minutes of operation, it was observed that the entire contact surface was coated with oxide. The scar obtained after another 5 minutes, with the same buffer, has a special shape, the oxidation wear area being limited to half of the loaded surface (sample 1002) – figure13.

3.2. Influence of the initial roughness on the fretting wear and of the friction coefficient

The minimum value of the surface wear must coincide with the minimum value of the surface roughness. A large number of wear measurements were performed with four roughnesses: $R_a = 0.015 \mu\text{m}$; $R_a = 0.045 \mu\text{m}$; $R_a = 0.075 \mu\text{m}$ and $R_a = 0.19 \mu\text{m}$. The average values of the volume of fretting worn material for the four roughnesses are

$$\begin{aligned} R_a = 0.015 \mu\text{m} &\rightarrow V_u = 7.0 \times 10^{-5} \text{ mm}^3 \rightarrow \mu = 0.038; \\ R_a = 0.045 \mu\text{m} &\rightarrow V_u = 7.0 \times 10^{-6} \text{ mm}^3 \rightarrow \mu = 0.050; \\ R_a = 0.075 \mu\text{m} &\rightarrow V_u = 3.7 \times 10^{-5} \text{ mm}^3 \rightarrow \mu = 0.038; \\ R_a = 0.190 \mu\text{m} &\rightarrow V_u = 1.0 \times 10^{-3} \text{ mm}^3 \rightarrow \mu = 0.078. \end{aligned}$$

Simultaneously with the production of fretting wear scars on the surface of the Ti-6Al-4V alloy samples, the coefficient of friction was also measured.

The effect of the running-in on the fretting wear behavior of the surface was also analyzed. This was done by using the same buffer for several successive tests.

In figure 14 are shown representative images of the running-in effect on the fretting wear behavior of the surface with the buffer from the previous determination, for three of the four roughnesses (samples 1077, 1065 and 1067).

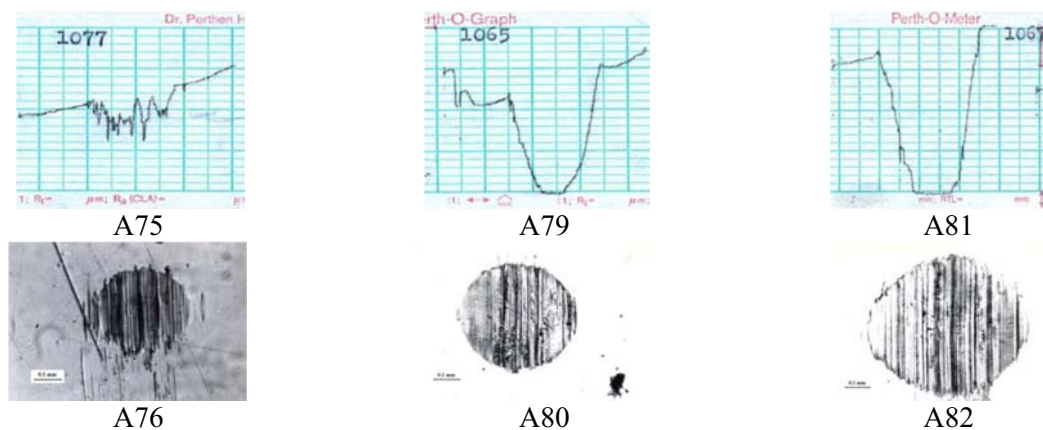


Figure 14. Effect of the running-in on the fretting wear behaviour of the surface with $R_a = 0.19 \mu\text{m}$, $t = 5 \text{ min}$, samples 1077, 1065 and 1067 (with the buffer from previous determination).

The existence of an optimal roughness can be explained either by an effect on the lubricant film or by a change in the mechanical properties of the surface. In this case, at the optimum roughness, the reduction of the h/σ ratio is compensated by increasing the wear resistance of the surfaces.

4. Conclusions

In the experimental conditions used, the fretting contact between the buffer and the sample was a point contact, which produced a fretting wear scar that evolved rapidly even during the short time considered (maximum 30 minutes).

The influence of the sample and buffer roughnesses on the initiation and evolution of the fretting wear scar was studied. The geometry of the test configuration allowed the investigation of finished surfaces at roughnesses $R_a = 0.015 \mu\text{m}$, $R_a = 0.045 \mu\text{m}$, $R_a = 0.075 \mu\text{m}$ and $R_a = 0.19 \mu\text{m}$.

From the determinations of fretting wear evolution in time under the experimental conditions used, it was found that in the case of the shortest experiment (5 minutes) the fretting wear scar is visible.

The recording of fretting scars allowed calculation of the volume of worn material by fretting and correlation with the value of the friction coefficient recorded during each test.

It has been found that there is a minimum of the wear curve resulted for roughness $R_a = 0.045 \mu\text{m}$.

A double-logarithmic evolution of fretting wear function of time was determined for different roughnesses analyzed. The used roughnesses caused not only a difference in the value of the scratch scar removal volume but also the appearance of wear scar (type of wear). Used roughnesses have caused not only a difference between the values of the worn volume of the fretting scar, but also of the wear scar appearance (type of wear).

After 3 seconds, in the case of surfaces with $R_a = 0.015 \mu\text{m}$, $R_a = 0.075 \mu\text{m}$ and $R_a = 0.19 \mu\text{m}$ ($t = 3 \text{ s}$), the fretting wear is of adhesive type (metallic shape with pronounced scratches). In the case of surfaces with $R_a = 0.045 \mu\text{m}$, the type of fretting wear is predominantly oxidative. During the running-in, the fretting wear velocity is reduced as a result of the surface conformation, and surfaces with $R_a = 0.075 \mu\text{m}$ and $R_a = 0.19 \mu\text{m}$ are undergoing in oxidative wear regime.

It has been observed that by increasing the operating time from 5 minutes to 30 minutes, the wear increases only with about 10%. It is worth noting the rapid reduction of the wear velocity over time, excepting the surface with roughness $R_a = 0.045 \mu\text{m}$, where in the first 3 seconds, between 25% and 50% of the wear occurs in 30 minutes. At surfaces with roughness $R_a = 0.045 \mu\text{m}$, a significant influence of the running-in was observed. After the first 5 minutes of operation, the entire contact surface is covered with oxide. The scar obtained after another 5 minutes, with the same buffer, has a special shape, the oxidative wear area being limited to half of the loaded surface.

In the experimental conditions $R_a = 0.015 \mu\text{m}$, $t = 5 \text{ min}$ and $R_a = 0.19 \mu\text{m}$, $t = 30 \text{ min}$ it is clearly observed the start of the fretting scars elongation in the sliding direction, as well as the typical W-shape of the transversal profile of the scar, noted in many of the papers published in the field.

It was found the existence of a minimum of the resulting wear curve for roughness $R_a = 0.045 \mu\text{m}$, but which surprisingly does not coincide with the minimum friction coefficient.

A mathematical relationship between the friction coefficient and wear can not be established.

References

1. Buciumeanu M., Crudu I., Palaghian L., Miranda A.S., Silva F.S., Influence of wear damage on the fretting fatigue life prediction of an Al7175 alloy, *International Journal of Fatigue*, vol. 31, 1278–1285, 2009.
2. Araujo J.A, Nowell D, Vivacqua R.C., The use of multiaxial fatigue models to predict fretting fatigue life of components subjected to different contact stress fields, *Fatigue & Fracture of Engineering Materials and Structures*, vol. 27, 967–978, 2004.
3. Madge J.J, Leen S.B, Shipway P.H., The critical role of fretting wear in the analysis of fretting fatigue, *Wear* vol. 263, 542–551, 2007.
4. Salerno G., Magnabosco R., de Moura Neto C., Mean strain influence in low cycle fatigue behaviour of AA7175-T1 aluminum alloy, *International Journal of Fatigue*, vol. 29, 829–835, 2007.
5. Szolwinsky M.P, Farris T.N., Observations, analysis and prediction of fretting fatigue in 2024-T351 aluminium alloy, *Wear*, vol. 221, 24–36, 1998.
6. Lykins C.D, Mall S., Jain V.K., Combined experimental–numerical investigation of fretting crack initiation, *International Journal of Fatigue*, vol. 23, 703–711, 2001.

7. Proudhon H., Fouvry S., Buffiere J.Y., A fretting crack initiation prediction taking into account the surface roughness and the crack nucleation process volume, *International Journal of Fatigue*, vol. 27, 569–579, 2005.
8. Landolt, D., Mischler, S., *Tribocorrosion of passive metals and coatings*, Woodhead Publishing Limited, 2011.
9. Fidrici V., Fouvry S., Kapsa P., Perruchaut P., Prediction of cracking in Ti-6Al-4V alloy under fretting-wear: use of the SWT criterion, *Wear*, vol. 259, 300–308, 2005.
10. Araujo J.A, Nowell D., The effect of rapidly varying contact stress fields on fretting fatigue, *International Journal of Fatigue*, vol. 24, 763–775, 2002.
11. Giannakopoulos A.E, Lindley T.C, Suresh S. Chenut C., Similarities of stress concentrations in contact at round punches and fatigue at notches: implications to fretting fatigue crack initiation, *Fatigue & Fracture of Engineering Materials & Structures*, vol. 23, 561–571, 2000.
12. Madge J.J., Leen S.B., Shipway P.H., The critical role of fretting wear in the analysis of fretting fatigue, *Wear*, vol. 263: 542–551, 2007.
13. Zheng J.F., Yang S., Shen M.X., Mo J.L., Zhu M.H., Study on rotational fretting wear under a ball-on-concave contact configuration, *Wear*, vol. 271, 1552-1562, 2011.
14. Fu, Y.Q., Wei, J., Batchelor, A.W., Some considerations on the mitigation of fretting damage by the application of surface-modification technologies, *Journal of Materials Processing Technology*, vol. 99, 231-245, 2000.
15. Kim K., Geringer J., Pellier J., Macdonald D.D., Fretting corrosion damage of total hip prosthesis: Friction coefficient and damage rate constant approach, *Tribology International*, vol. 60, 10–18, 2013.
16. Batchelor A. W., Stachowiak G. W., Stachowiak G. B., Control of fretting friction and wear of roping wire by laser surface alloying and physical vapour deposition coatings, *Wear*, vol. 152, 127-150, 1992.
17. Geringer J., Forest B., Combrade P., Fretting-corrosion of materials used as orthopaedic implants, *Wear*, vol. 259, 943–951, 2005.
18. Geringer J., Macdonald D.D., Modeling fretting-corrosion wear of 316L SS against poly(methyl methacrylate) with the Point Defect Model: Fundamental theory, assessment, and outlook, *Electrochimica Acta*, vol. 79, 17– 30, 2012.
19. Garcia D.B., Grandt A.F. Jr., Fractographic investigation of fretting fatigue cracks in Ti–6Al–4V, *Engineering Failure Analysis*, vol. 12, 537–548, 2005.
20. Magaziner R.S., Jain V.K., Mall S., Wear characterization of Ti-6Al-4V under fretting – reciprocating sliding conditions, *Wear*, vol. 264, 1002-1014, 2008.